Chapter

Landslide Potential Evaluation Using Fragility Curve Model

Yi-Min Huang, Tsu-Chiang Lei, Bing-Jean Lee and Meng-Hsun Hsieh

Abstract

The geological environment of Taiwan mainly contains steep topography and geologically fragile ground surface. Therefore, the vulnerable environmental conditions are prone to landslides during torrential rainfalls and typhoons. The rainfall-induced shallow landslide has become more common in Taiwan due to the extreme weathers in recent years. To evaluate the potential of landslide and its impacts, an evaluation method using the historical rainfall data (the hazard factor) and the temporal characteristics of landslide fragility curve (LFC, the vulnerability factor) was developed and described in this chapter. The LFC model was based on the geomorphological and vegetation factors using landslides at the Chen-Yu-Lan watershed in Taiwan, during events of Typhoon Sinlaku (September 2009) and Typhoon Morakot (August 2009). The critical hazard potential (*Hc*) and critical fragility potential (*Fc*) were introduced to express the probability of exceeding a damage state of landslides under certain conditions of rainfall intensity and accumulated rainfall. Case studies at Shenmu village in Taiwan were applied to illustrate the proposed method of landslide potential assessment and the landslide warning in practice. Finally, the proposed risk assessment for landslides can be implemented in the disaster response system and be extended to take debris flows into consideration altogether.

Keywords: landslide, fragility, landslide potential, probabilistic model

1. Introduction

Taiwan is on the path of western Pacific typhoon path and on the circum-Pacific earthquake belt, indicating that Taiwan suffered from two or more natural disasters, which was the highest in the world [1]. Besides, most of the land in Taiwan, about 70% of total area, is hillside. Given the conditions of increasing impacts of climate change and extreme weathers, the rainfall-induced landslide has become a serious issue in Taiwan.

Most landslide researches used the landslide susceptibility analysis (LSA) to develop landslide evaluation model [2]. The LSA models basically use factors and observed data to construct the description of landslides. The factors include rainfall intensity, accumulated rainfall, slope degree, vegetation, etc. The common models developed for landslide hazard or landslide evaluation are usually deterministic analysis, including the traditional slope stability analysis [2]. Recently, a novel concept of applying probability to landslide evaluation had been proposed.

The fragility curves, which are commonly used in the earthquake-induced structure analysis, had been adopted to represent the probability of landslide [3–5]. The process of applying fragility curve to landslide evaluation is to consider and estimate the recurrence and the probability of exceedance of a damage level for a landslide [3, 4].

In this chapter, the preparation of landslide fragility curves was introduced. The procedure of developing the landslide fragility curve (LFC) model was the researches of rainfall-induced shallow landslide in the past years [2–5]. The proposed LFC model considered the impacts of rainfall and the vulnerability of environment. Instead of using one-variable triggering factor (rainfall intensity or accumulation) in the previous research [2], the newly improved LFC model used bivariate approach in the model [3, 4]. The improved LFC model introduced the landslide fragility surface (LFS) by considering the influence of both rainfall intensity and accumulation at the same time [4, 5].

The spatial statistics and geographic information system (GIS) were used for data processing. The data of each factor used in the model was further divided into groups. Classification of factors represented the environmental characteristics of a specific area. The analysis basis was conducted spatially on the slope units, which are topographically defined as the parts of a watershed [5]. With the LFS model, the risk assessment of landslide then was analyzed in association with the rainfall hazard potential [4, 5]. The Shenmu area of Chen-Yu-Lan watershed was selected as the study area, and historical cases were used to illustrate the application of LFS model.

2. The factors and environmental database

When considering the factors to be used in the landslide problem, these factors are generally classified as triggering and environmental factors [6–8]. Among these factors, the rainfall is usually the major concern, and for environmental vulnerability, many factors can be chosen from. Not every chosen environmental factor can be used in developing a landslide model because of (1) few data in the database, (2) lack of data, and (3) low influence in the model. In this chapter, the cumulative rainfall and maximum hourly rainfall (rainfall intensity) were used for triggering factors, whereas slopes, slope aspects, landslide area, incremental landslide area, ratio of incremental landslide area, normalized difference vegetation index, distance to the nearest river, and geology were used for environmental factors of hillside slope in the study. A GIS database to describe landslide areas was created and was later applied in developing the proposed fragility curve model. These indexes, factors, and symbol definitions are explained in the following:

1. Maximum rainfall intensity (I_{max}): the maximum rainfall intensity is the rainfall in the form of rainfall per unit time. In this study, I_{max} refers to the maximum hourly rainfall (**Figure 1**) and was used as a triggering factor for LFC model.

2. Effective accumulated rainfall (R_{te}): the R_{te} is defined as the accumulated rainfall before the maximum rainfall intensity in a continuous raining event (**Figure 1**), by considering the influence of antecedent 7-day rainfall.

3. Hillside slope (S): the dynamic behavior of the landslide has close relationship with the slope. Hence, the degree of slope may be a prominent factor of triggering landslides. In this study, the slope was classified based on the Soil and

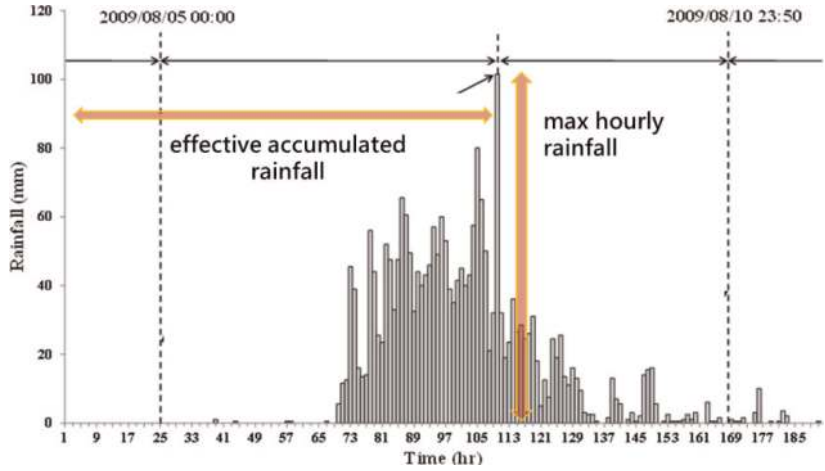

Figure 1.
The definition of rainfall indices: I_{max} and R_{te} (modified after [2–4]).

Water Conservation Bureau manual [9]. There are seven slope levels of 5% or less, 5–15%, 15–30%, 30–40%, 40–55%, 55–100%, and slope exceeding 100%. The slopes <15% are recognized as flat ground or very gentle slopes and not included in this study. Slopes of levels 3–7 were studied in the landslide model.

4. Slope aspect (A): the slope aspect represents the vulnerable directions of occurring landslide when given a known topography. This factor may represent the "weak" aspect of a slope in terms of landslide.

5. Landslide area (LA): observing the landslide distribution through image classification results can obtain the information about the land cover change. The change from events of Typhoon Sinlaku (in 2008) and Typhoon Morakot (in 2009) was identified using GIS software.

6. Incremental landslide area (IA): to understand the landslide increment, the images before and after a landslide were considered. The landslides are classified into five categories (shown in **Figure 2**): (1) the original landslide area (number 1 + 2), (2) the original landslide area extension (number 2), (3) new landslide area on single period (number 3), (4) new landslide area on pre-/post periods (number of 2 + 3), and (5) vegetation restoration area (number of 1). In this study, the new landslide area on pre-/post periods (number of 2 + 3) was considered.

7. Ratio of incremental landslide area (RIL): to obtain the ratio of incremental landslide area, this study used the incremental landslide area from image of two periods to determine this factor.

8. Vegetation index (N): to determine the density of vegetation on a patch of land, researchers must observe the distinct colors (wavelengths) of visible and near-infrared sunlight reflected by the plants [10]. Nearly almost satellite vegetation indices employ the difference formula, $(NIR - R)/(NIR + R)$ [11], to quantify the density of plant growth on the earth—the subtraction of near-infrared radiation (NIR) and red radiation (R) divided by the addition of near-infrared radiation and red radiation. The result of this formula is called the normalized difference vegetation index (NDVI). The values for NDVI in this study were obtained from SPOT image. The range of NDVI is −1 to 1.

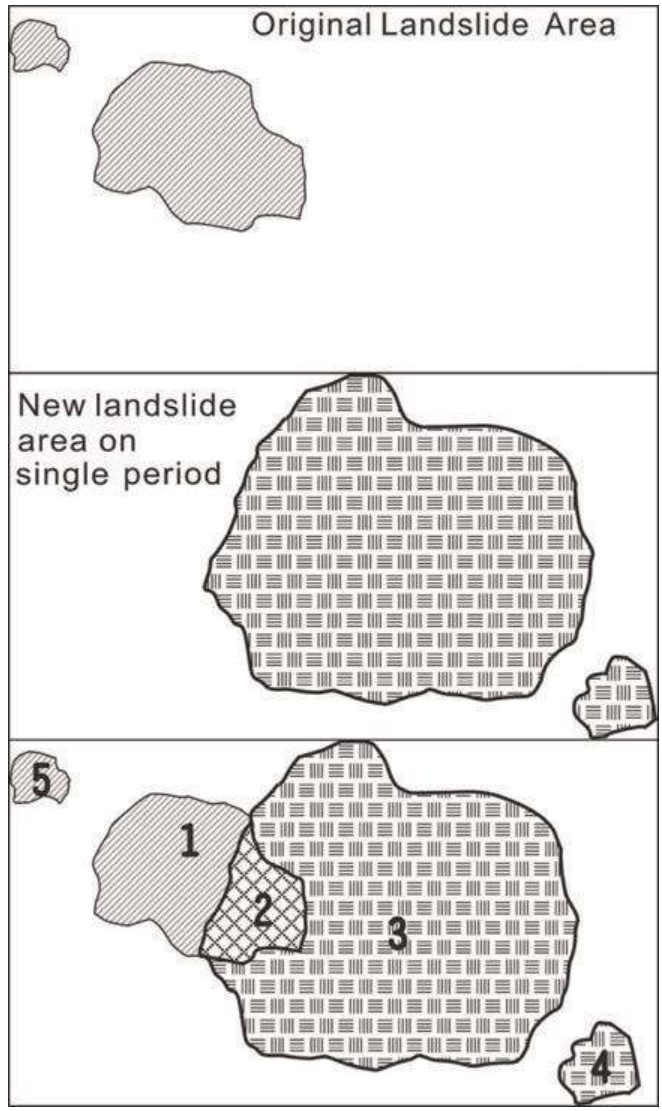

Figure 2.
Concept of mapping landslide area change: differences between two periods of SPOT image [2].

9. Distance to the nearest river (R): the landslide may be triggered due to the erosion by the river at the toe section. The distance to the river reflects the potential of landslide contributed from the river system.

10. Geology (G): the geological time scale of the area and the rock types of the site were combined into consideration as the geology factor. In the past studies, the geology-related information (like the rock types and rock strength) was not usually available. Therefore, to simplify the classification, the geological time scale was chosen to represent the possible influence of geology.

3. Study area and material

To explain the landslide fragility model, the Shenmu area in Taiwan was used as a case to demonstrate the development of LFC of a given site. The Shenmu area locates in the watershed of Chen-Yu-Lan River. Chen-Yu-Lan watershed is at the central part of Taiwan (**Figure 3**). The Chen-Yu-Lan River originates from the

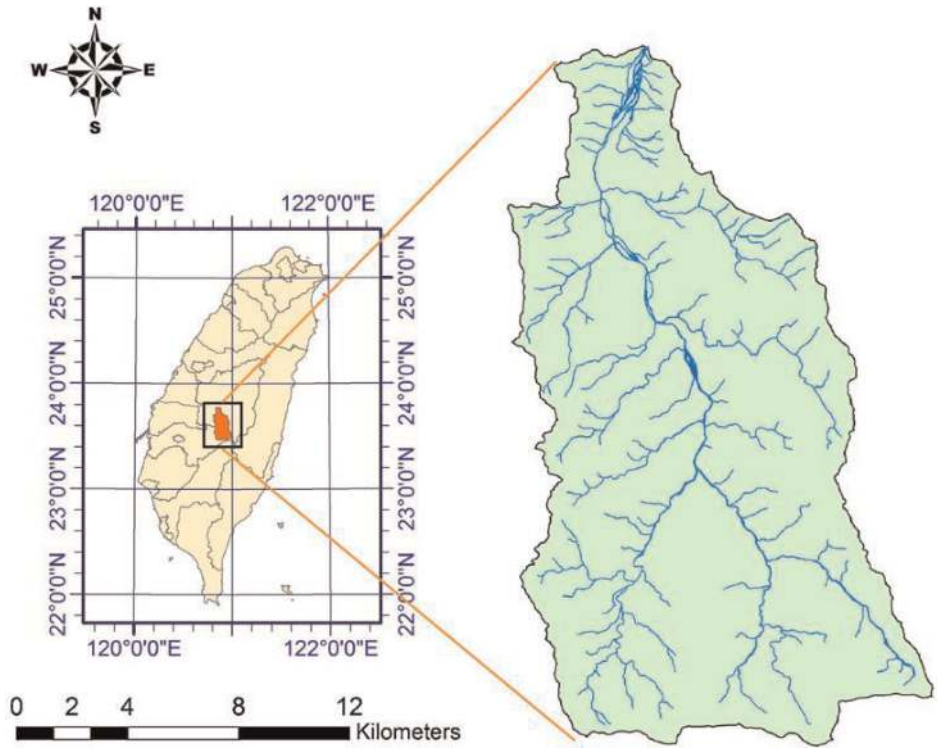

Figure 3.
Chen-Yu-Lan watershed [2].

north peak of Yu Mountain and is one of the upper rivers of the Zhuoshui River system, which is the largest river system in Taiwan. Chen-Yu-Lan River has a length of 42.4 km with an average declination slope of 5%, and its watershed area is about 450 km^2. This area was fragile after the Chi-Chi Earthquake (occurred on September 21, 1999).

The Shenmu area is a location where debris flows frequently occurred [5]. The local village is adjacent to the confluence of three streams: Aiyuzi Stream (DF226), Huosa Stream (DF227), and Chushuei Stream (DF199). In Shenmu, the debris flows usually occurred at the Aiyuzi Stream due to its shorter length and large landslide area (**Table 1**) in its upstream [5]. **Figure 4** shows the terrain of three streams.

In addition to the basic terrain data of Shenmu area, the hydrologic and geographic factors are needed in modeling. To obtain these factors, an environment database of Chen-Yu-Lan watershed was prepared. Among the data collection, the landslide increment (i.e., new landslides) after a rainfall event was also obtained by image processing method in this study.

To develop the LFC model, the local environmental data was collected for the study area, and GIS was used to process the data. The environment database of Chen-Yu-Lan watershed includes data of geology, geological layers, rock property, slope and slope aspects, and DEM, as shown in **Figures 5–8**.

Debris flow no.	Stream	Length (km)	Catchment area (km^2)	Landslide area (km^2)
DF199	Chushuei stream	7.16	8.62	0.33
DF227	Huosa stream	17.66	26.20	1.49
DF226	Aiyuzi stream	3.30	4.00	1.00

Table 1.
The landslide area in Shenmu after 2009 [5].

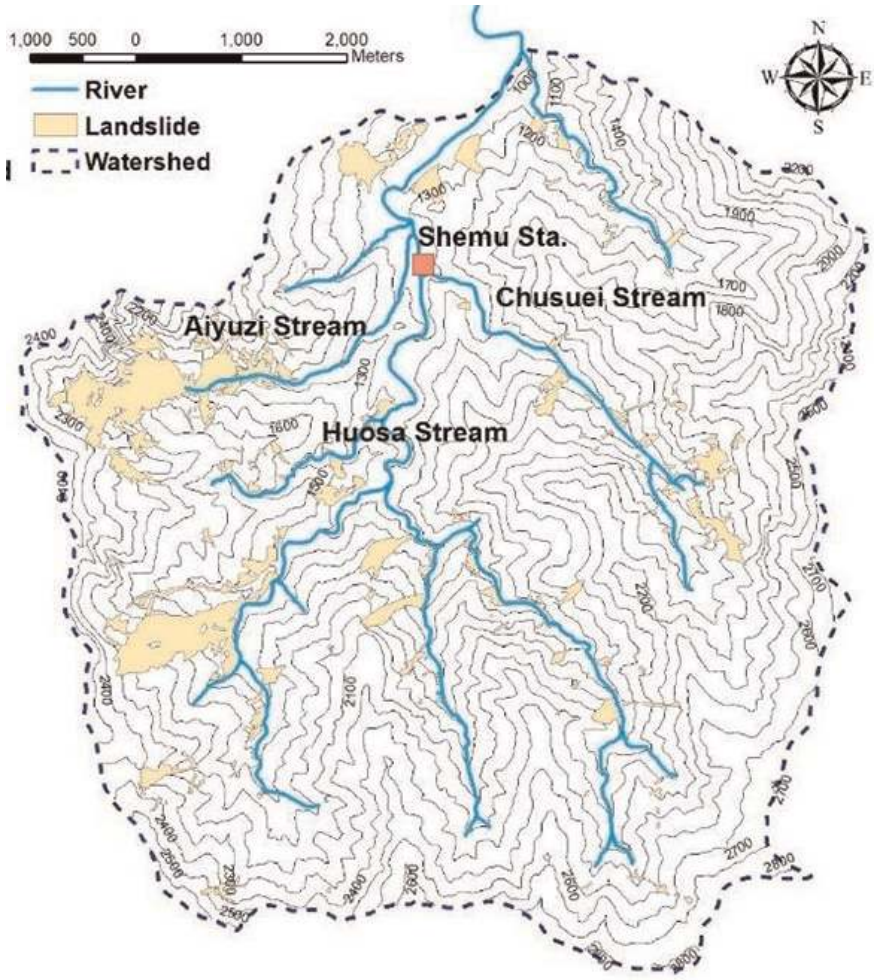

Figure 4.
The terrain and landslide areas of Shenmu area.

The new landslide areas (**Figures 9** and **10**) were identified by using pre- and post-event satellite images of Typhoon Sinlaku in 2008 and Typhoon Morakot in 2009 (**Table 2**). These landslide areas were used for later LFC model analysis. Another important factor in the LFC model is the vegetation conditions. The information of vegetation status was also obtained by image processing the same as the determination of new landslides.

In addition to the hydrologic and geographic data, the landslide triggering factors were also considered in data preparation. **Table 3** defines the rainfall indices. It should be noted that the effective accumulated rainfall was calculated by including the antecedent 7-day accumulated rainfall. The antecedent 7-day accumulated rainfall is the total weighted rainfall counted from the 7-day duration before the starting of current rainfall event. Take Typhoon Sinlaku (September 11–16, 2008) for example. The starting date of Typhoon Sinlaku was September 11, 2008, and the antecedent 7-day accumulation rainfall was the total weighted rainfall during September 3 to September 10, as described as *Ra* in **Table 3**.

Figures 11 and **12** show the rainfall interpolation of the events of Typhoon Sinlaku (September 11–16, 2008) and Typhoon Morakot (August 5–10, 2009). The red spots in the figure are the locations of rainfall stations. It was noted that the rainfall intensity and the cumulative rainfall of event of Typhoon Morakot were much higher than those of Typhoon Sinlaku. Both events had caused serious landslides in the central Taiwan.

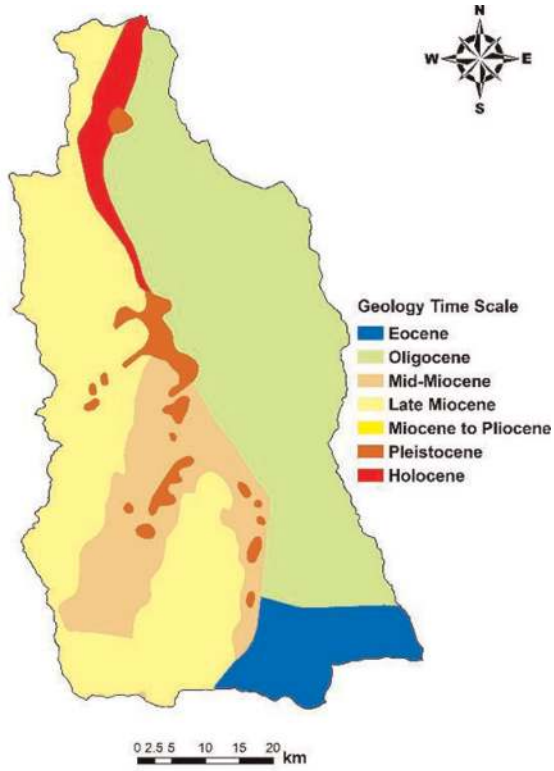

(a)

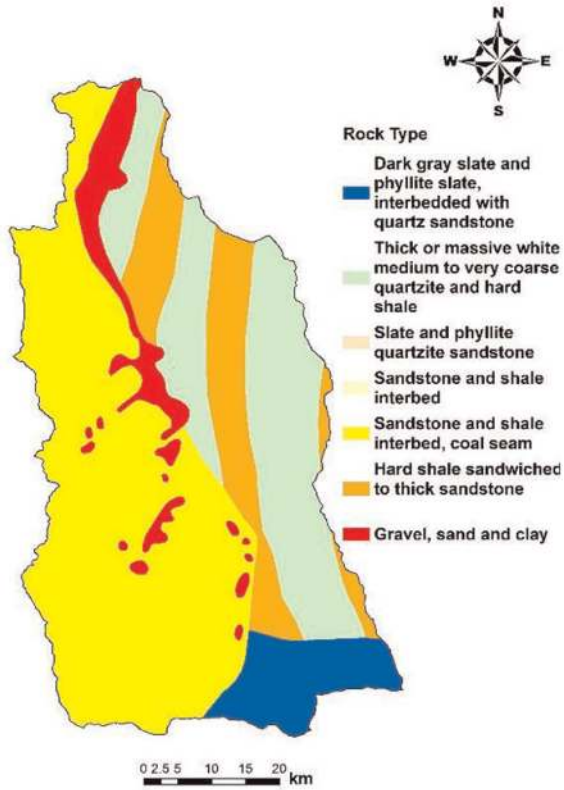

(b)

Figure 5.
Chen-Yu-Lan watershed: (a) geological time scale and (b) rock types.

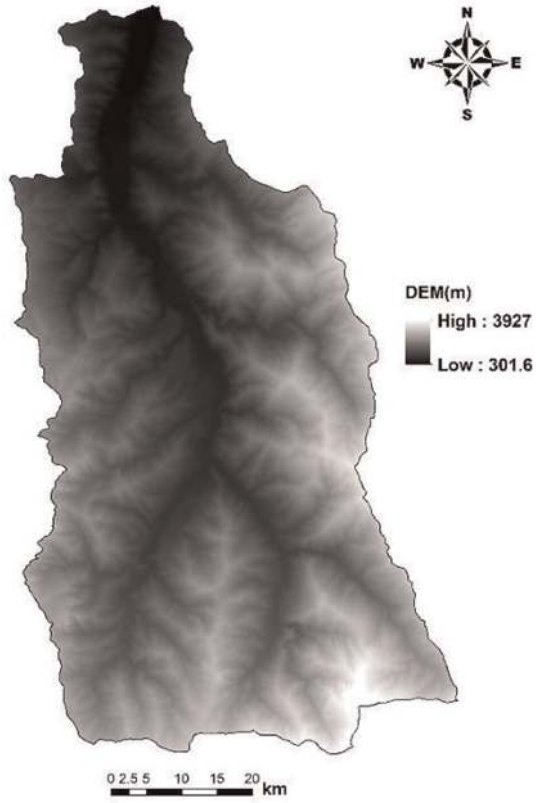

Figure 6.
Five-meter DEM of Chen-Yu-Lan watershed (after [2]).

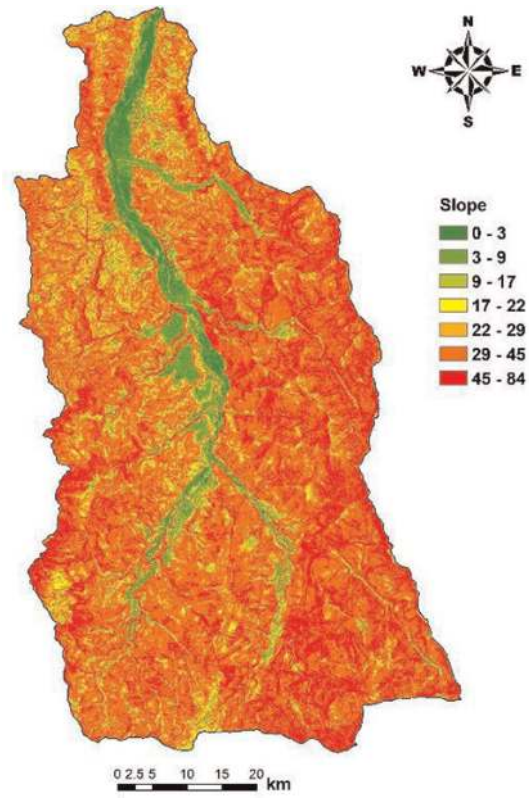

Figure 7.
The slope of Chen-Yu-Lan watershed.

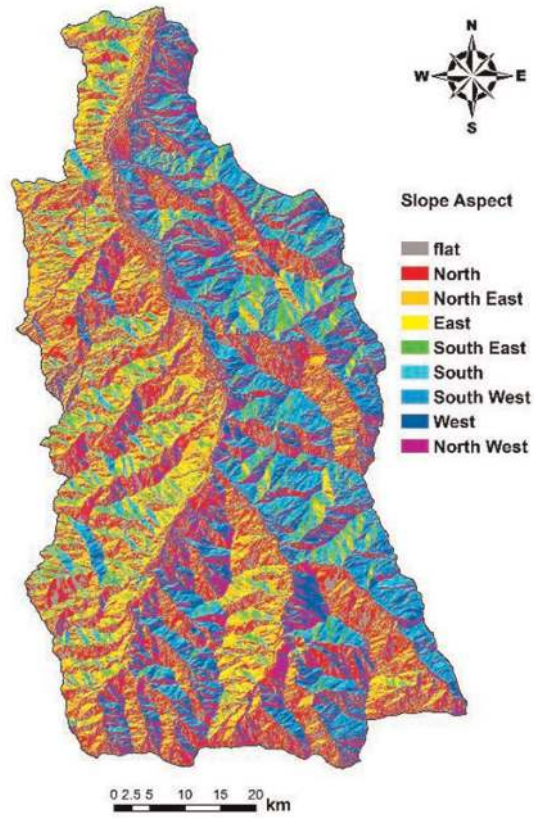

Figure 8.
The slope aspects of Chen-Yu-Lan watershed.

Finally, the database was used to analyze the study area on the basis of slope units. The slope unit was defined as in **Figure 13**. A slope unit is defined as one slope part or the left/right part of a watershed. Slope units can be topologically divided by the watershed divide and drainage line, with the help of GIS tool [12]. The application of slope unit in the development of LFC was based on the physical interpretation of slopes in the mountain area. The environmental database was applied in accordance with the slope units at the site of interest. **Figure 14** shows the slope unit distribution (total 5872 units) of Chen-Yu-Lan watershed.

4. Development of empirical landslide fragility model

To develop the empirical landslide fragility model, a probability distribution was chosen to describe the potential of landslide fragility. When the probability distribution was determined, the parameters of probability, the median and standard deviation, were obtained by fitting the data from the environmental database and the landslide areas. The use of slope unit was adopted here, and the classification of environmental factors was applied to represent the conditions of landslide given rainfall intensity and accumulated rainfall. The procedure of developing the empirical landslide fragility curve was described in the following.

4.1 Probability distribution of LFC

The fragility analysis is usually used to describe the potential of hazard in terms of potential levels or probability of exceedance of a level. To describe the probability

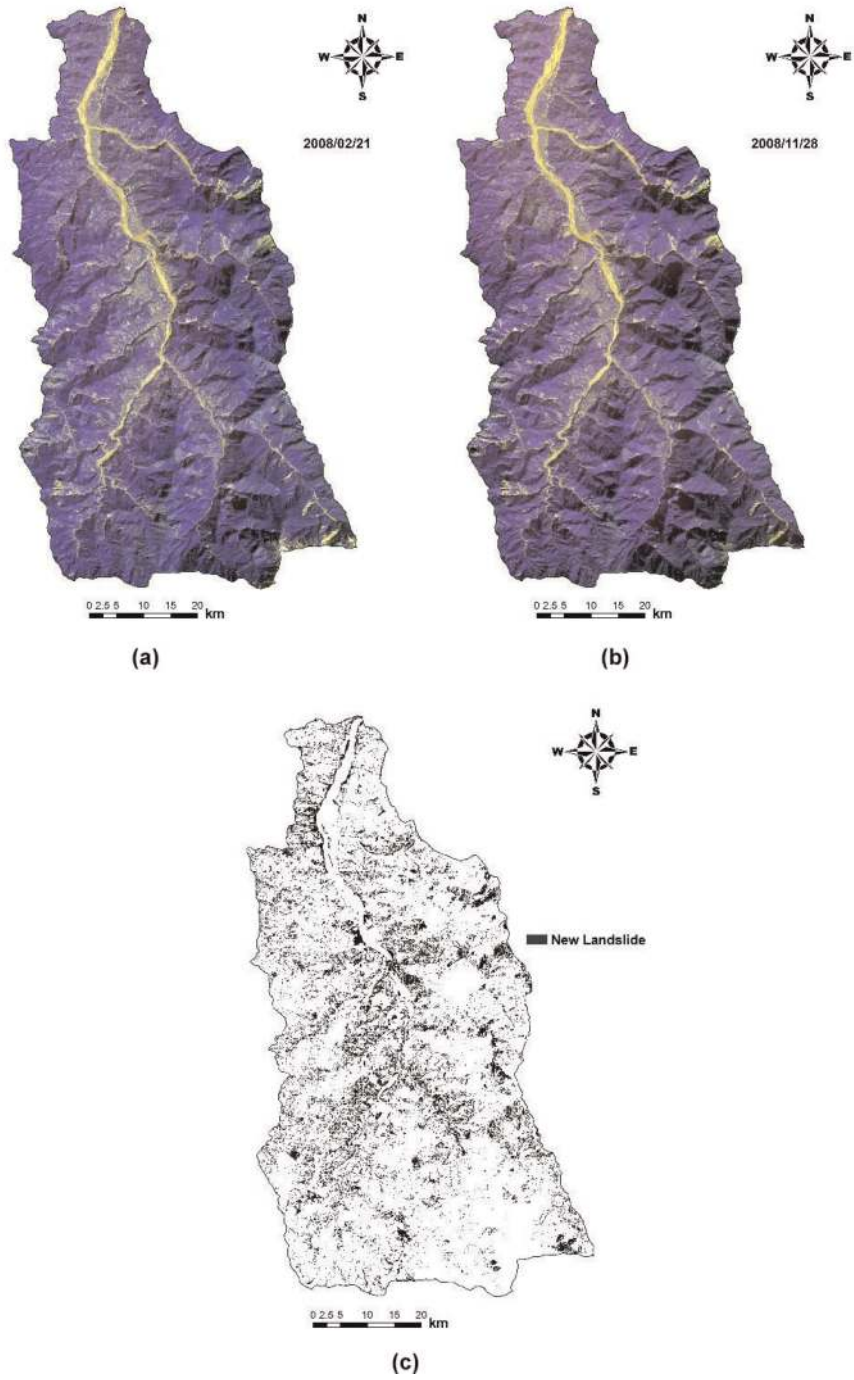

Figure 9.
Satellite images of pre- (a) and post-event (b) Typhoon Sinlaku and the new landslide areas (c) in Chen-Yu-Lan watershed.

about a hazard fragility, a feasible probability distribution can be assumed and applied in the model. The fragility curve of landslide, therefore, was assumed to be a lognormal distribution [12, 13]. The lognormal distribution can be constructed simply by the values of median and lognormal standard deviation and are called bivariate parameters (Eq. (1)):

$$f_j\left(x; c_j, \zeta_j\right) = \frac{1}{\sqrt{2\pi}\zeta_j x} e^{-\frac{1}{2}\left(\frac{ln\left(x/c_j\right)}{\zeta_j}\right)^2} \quad (1)$$

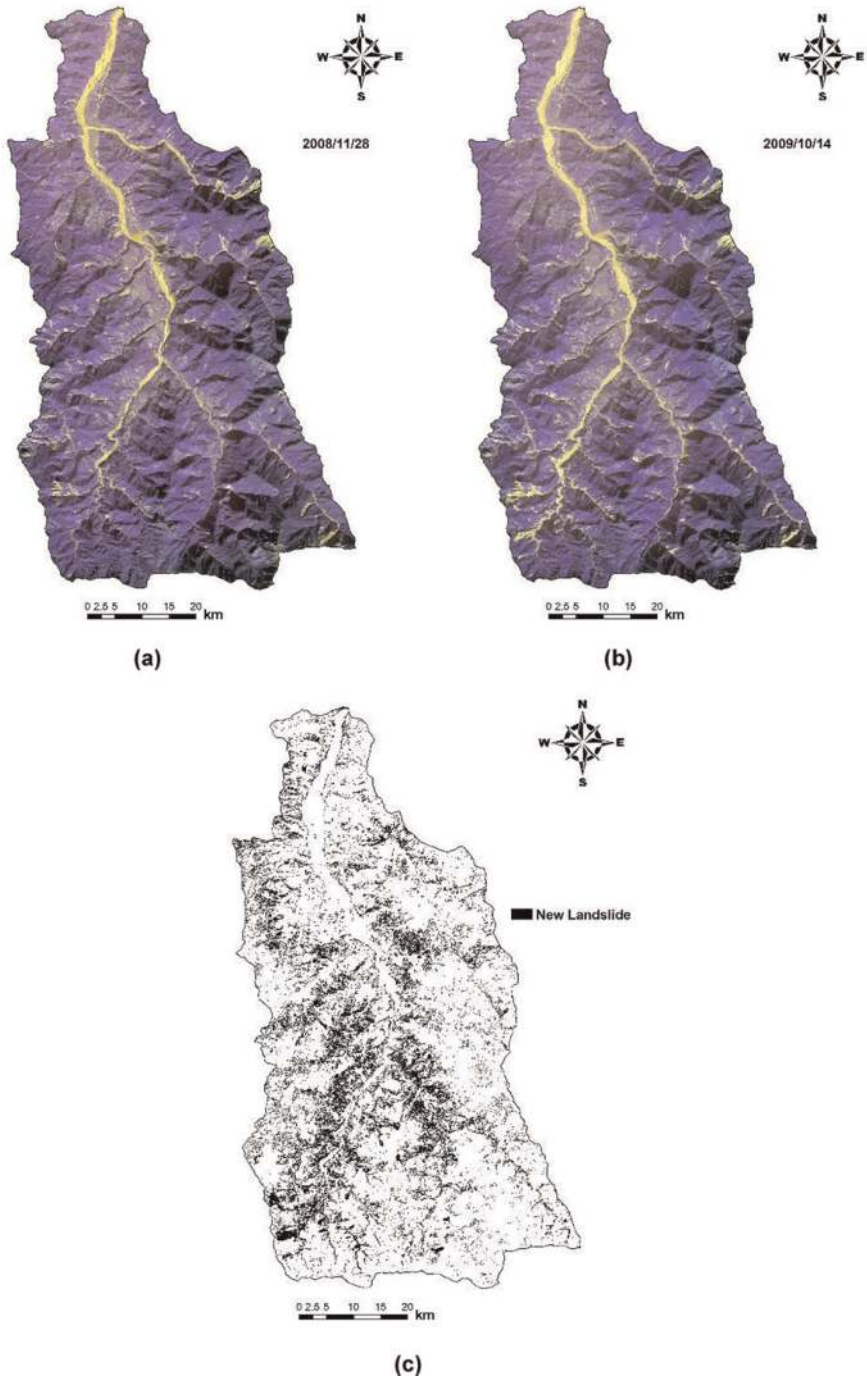

Figure 10.
Satellite images of pre- (a) and post-event (b) Typhoon Morakot and the new landslide areas (c) in Chen-Yu-Lan watershed.

where f_j is the probability density function of lognormal distribution, c_j is the median, ζ_j is the log-standard deviation, and x is the variable. The cumulative distribution of Eq. (1) is used as the fragility curve. The cumulative density function of lognormal distribution is expressed as Eq. (2):

$$F_j\left(x;c_j,\zeta_j\right) = \frac{1}{2} + \frac{1}{2}\, erf\left[\frac{ln\left(x/c_j\right)}{\zeta_j\sqrt{2}}\right] \tag{2}$$

Watershed	Event	Image time	Satellite	Incremental area (km^2)
Chen-Yu-Lan 448.14 km^2	Pre-Sinlaku	February 21, 2008	SPOT5	9.52 (2.12%)
	Post-Sinlaku	November 28, 2008	SPOT5	
	Pre-Morakot	November 28, 2008	SPOT5	10.21 (2.28%)
	Post-Morakot	October 14, 2009	SPOT5	

Table 2.
Satellite images of events at Chen-Yu-Lan watershed.

Index	Symbol	Definition
Max. hourly rainfall	I_{max}	The maximum hourly rainfall in a rainfall event
Effective accumulated rainfall	R_{te}	The antecedent 7-day accumulated rainfall (with reduction factor of 0.7*) before the starting of current event and the accumulated rainfall before the max. hourly rainfall in current event

**Antecedent 7-day accumulated rainfall (R_a) can be calculated by $R_a = \sum_{i=1}^{7} 0.7^i R_i$, where R_i is the daily rainfall of the ith day before.*

Table 3.
The rainfall indices.

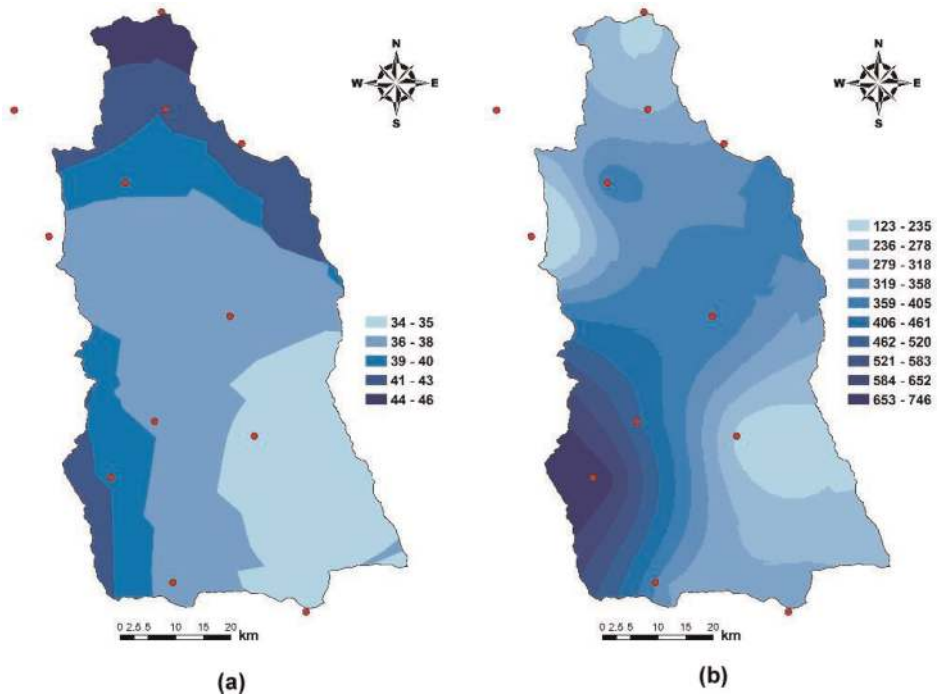

Figure 11.
Rainfall indices of Typhoon Sinlaku: (a) I_{max} and (b) R_{te}.

Eq. (2) represents the *j*th fragility, and *erf()* is the Gaussian error function. When the median and log-standard deviation are determined, the fragility curve of *j*th level can be obtained. The maximum likelihood estimation (MLE) can be applied to determine the median and log-standard deviation [13]. The aforementioned equations are suitable for one-variable estimation model.

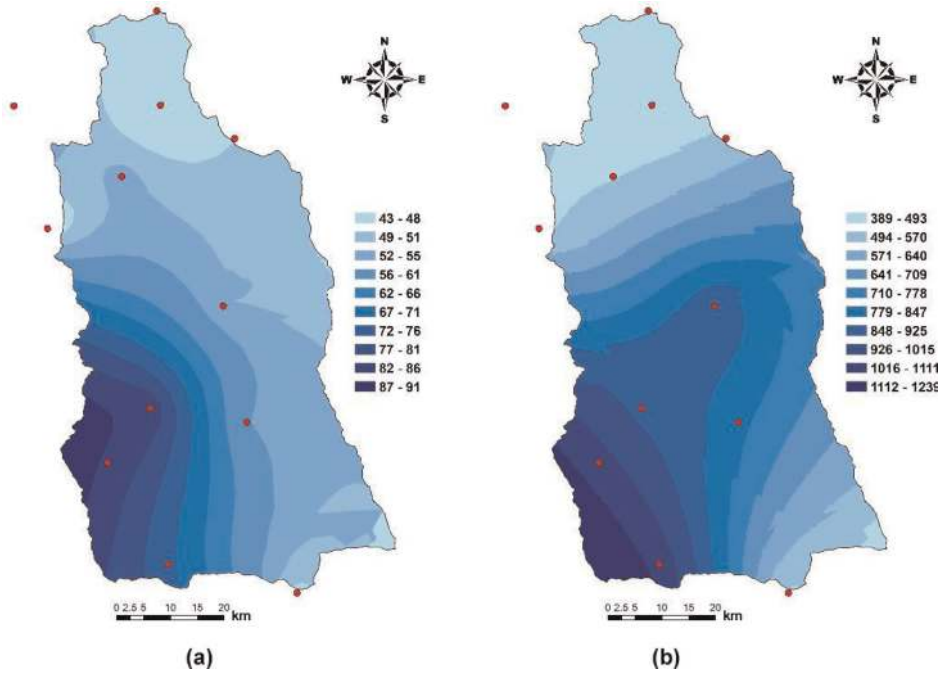

Figure 12.
Rainfall indices of Typhoon Morakot: (a) I_{max} and (b) R_{te}.

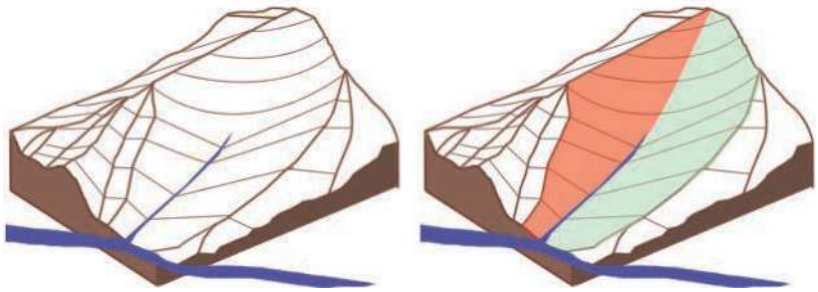

Figure 13.
Slope unit delineation, the left and right slope units of a watershed [3, 4].

Since both the rainfall intensity and rainfall accumulation contribute to the probability of triggering a landslide, the bivariate lognormal distribution was applied in the developing LFC model [4, 14], as in Eq. (3):

$$f_j(x,y) = \frac{1}{2\pi y \zeta_{xj}\zeta_{yj}\sqrt{1-\rho_j^2}}\ exp\left\{-\frac{1}{2\left(1-\rho_j^2\right)}\left[\frac{ln\left(x/c_{xj}\right)^2}{\zeta_{xj}^2} - 2\rho_j\frac{ln\left(x/c_{xj}\right)ln\left(y/c_{yj}\right)}{\zeta_{xj}\zeta_{yj}} + \frac{ln\left(y/c_{yj}\right)^2}{\zeta_{yj}^2}\right]\right\} \tag{3}$$

where $-\infty < x, y, \zeta_{xj}, \zeta_{yj} < \infty$, $c_{xj} > 0$, $c_{yj} > 0$, and $-1 < \rho_j < 1$. In Eq. (3), x and y are maximum hourly rainfall and effective accumulated rainfall, respectively; c_{xj} and c_{yj} are the median; ζ_{xj} and ζ_{yj} are log-standard deviation; ρ_j is the correlation coefficient of x and y. Because the maximum hourly rainfall and the effective accumulated rainfall are treated independently, the ρ_j is zero. Thus, the cumulative density function of Eq. (3) becomes as follows:

$$F_j\left(x, y; c_{xj}, c_{yj}, \zeta_{xj}, \zeta_{yj}\right) = \frac{1}{4}\left[1 + erf\left(\frac{ln\left(x/c_{xj}\right)}{\zeta_{xj}\sqrt{2}}\right)\right]\left[1 + erf\left(\frac{ln\left(y/c_{yj}\right)}{\zeta_{yj}\sqrt{2}}\right)\right] \quad (4)$$

Eq. (4) represents the j-th fragility curve of landslide, including four fragility parameters. The cumulative density function of Eq. (4) is a fragility surface of probability.

The parameters in Eq. (4) can be obtained by using the least square estimate. When the landslide locations and areas are available, meaning the classification of landslide based on the factors (see next section), the fragility curve of landslide (a surface) of a specific classification can be determined.

4.2 Classification of factors

The environmental factors, geology, slope, distance to river, slope aspect, and vegetation index, were classified into levels in order to group similar slope units. The triggering factors of rainfall intensity and effective accumulated rainfall were also redistributed onto slope unit scale. These factors were classified into groups, i.e., two groups of G, three of S, two of R, two of A, and two of N (**Tables 4–8**),

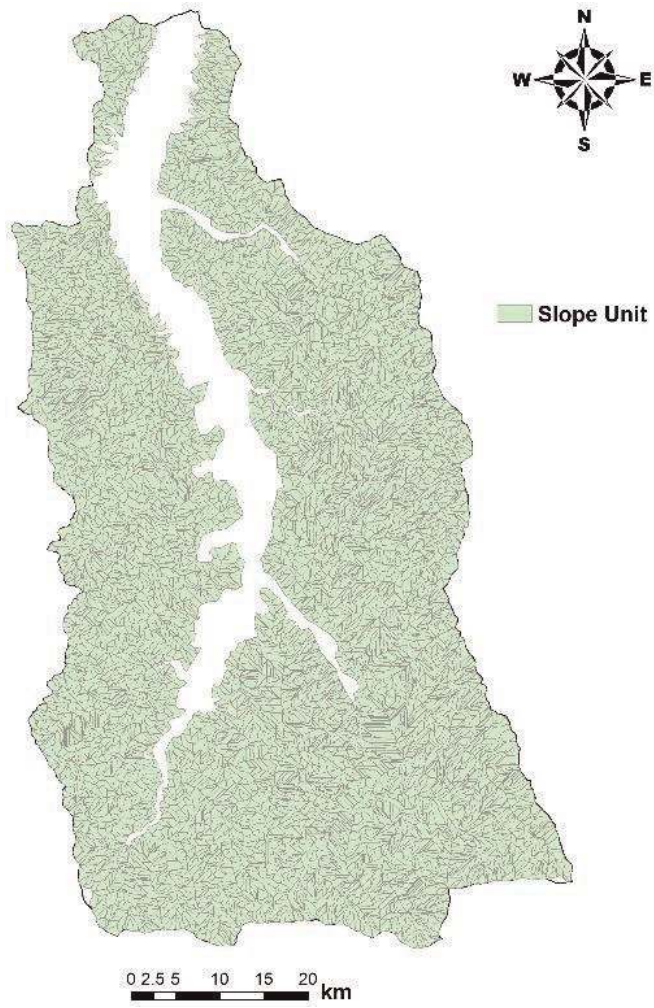

Figure 14.
The slope units of Chen-Yu-Lan watershed.

based on the available data and appropriate judgment to simplify the process. There were total of 48 combinations of classification, as described below.

4.2.1 Geology

The geology is an important factor when considering the potential of landslide. However, the geological conditions, like soil layer depth, rock type, and strength at the site, are not usually available to researchers. Therefore, a simplified step can be used at the geology time scale to generally represent the older and younger stratum of the study area. For Chen-Yu-Lan watershed, the rock type of the area was first used to highlight the geological time scale. The same geology era contained different rock formations, and the factor of geology was classified into two groups, as shown in **Table 4** and **Figure 15**. It was noted that there are 1798 slope units of G1 and 2463 slope units of G2.

4.2.2 Hillside slope

Based on the Soil and Water Conservation Bureau manual, the hillside slope is classified as seven levels. In the fragility model, level 3 to level 7 slopes were considered and simply further classified as three groups, as shown in **Table 5**. **Figure 16** shows the classification results in the Chen-Yu-Lan watershed, and 137 slope units were classified as S1, 827 as S2, and 3297 as S3.

4.2.3 Distance to nearest river channel

The distance to the nearest river channel was classified into two groups, with the threshold value of 300 m. **Table 6** and **Figure 17** show the classification results, in which there are 2482 and 1779 slope units of R1 and R2, respectively.

Classification	Geology time scale	Rock type
G1	Eocene	Dark gray slate and phyllite slate, interbedded with quartz sandstone
	Eocene	Slate and phyllite quartzite sandstone
	Oligocene	Hard shale sandwiched to thick sandstone
	Oligocene	Thick or massive white medium to very coarse quartzite and hard shale
G2	Miocene	Hard shale, slate, phyllite sandstone
	Mid-Miocene	Sandstone and shale interbed, coal seam
	Late Miocene	Sandstone and shale interbed, coal seam
	Miocene to Pliocene	Sandstone and shale interbed, coal seam
	Pliocene	Shale, sandy shale, mudstone
	Pliocene	Sandstone, mudstone, shale interbed
	Pliocene to Pleistocene	Gravel
	Pleistocene	Gravel, sand, and clay

Table 4.
The geology classification.

Classification	SWCB slope level	Technical regulations for soil and water conservation	
		Slope range	degree (°)
S1	3	15% < S ≦ 30%	8.53 < S ≦ 16.70
	4	30% < S ≦ 40%	16.70 < S ≦ 21.80
S2	5	40% < S ≦ 55%	21.80 < S ≦ 28.81
S3	6	55% < S ≦ 100%	28.81 < S ≦ 45.00
	7	S > 100%	S > 45.00

Table 5.
The slope classification.

Classification	Definition	Distance (m)
R1	Close	≤300 m
R2	Not close	>300 m

Table 6.
The classification of distance to river.

Classification	Definition
A1	Weak aspect: the four slope aspects of higher ratio of incremental landslide area. In this study, A1 are E, SE, S, and SW
A2	Strong aspect: the four slope aspects of lower RIL. In this study, A2 are W, NW, N, and NE

Table 7.
The classification of slope aspects.

Image process		Classification	
		Low vegetation	Mid-to-high vegetation
		$-1 < NDVI \leqq NDVIc^*$	$NDVIc^* < NDVI \leqq 1$
Pre-event image	Barren land	N1	N1
	Non-barren land	N1	N2

**NDVIc is the threshold value to classify low and mid-to-high vegetation index. In this study, the NDVIc was −0.35.*

Table 8.
The vegetation classification.

4.2.4 Slope aspects

The slope aspect was considered in the beginning to distinguish the range of frequent landslide on a given mountain slope. There are eight slope aspects (**Figure 18**) used in the study that were grouped into two classes as shown in **Table 7** and **Figure 19**, in which there are 2051 and 2210 slope units of A1 and A2, respectively.

4.2.5 Vegetation index

The land cover status was also an important factor when estimating the landslide potential. The normalized difference vegetation index was used to represent the

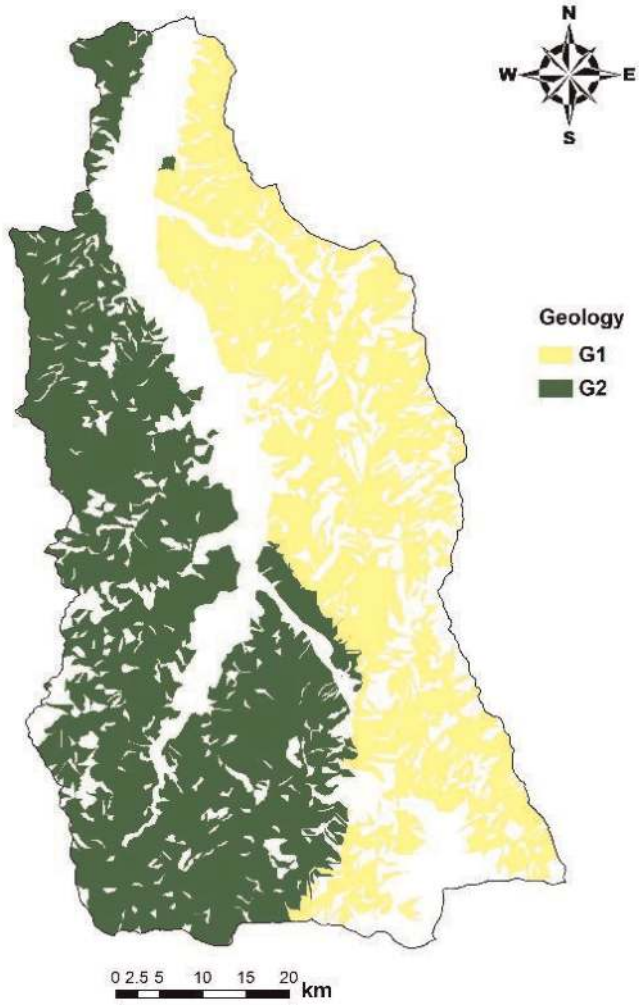

Figure 15.
The geology classification of Chen-Yu-Lan watershed.

land cover status of a given site. Satellite images of SPOT (February 21, 2008, November 28, 2008, and October 14, 2009) were used to calculate the NDVI of the ground surface, and an empirical NDVI threshold was applied to classify barren land and non-barren land. **Table 8** summarized the classification, and **Figure 20** shows the results, in which there are 2765 and 1496 slope units of N1 and N2, respectively.

4.2.6 Maximum rainfall intensity and effective accumulated rainfall

The rainfall data from Typhoon Sinlaku in 2008 and Typhoon Morakot in 2009 was applied to obtain the rainfall intensity and effective accumulated rainfall in the Chen-Yu-Lan watershed. The hourly rainfall data measured at the surrounding weather stations was used to get the rainfall of each slope unit by interpolation. **Figures 21** and **22** show the rainfall distribution during the two typhoon events.

4.2.7 Landslide area

Based on the site investigation in the past after typhoon events, the expected average landslide volume (V) was set as V = 6000 m^3. By applying the relationship of $V = 0.2 \times A^{1.3}$ [15], the landslide area on the slope can be obtained. Therefore, in

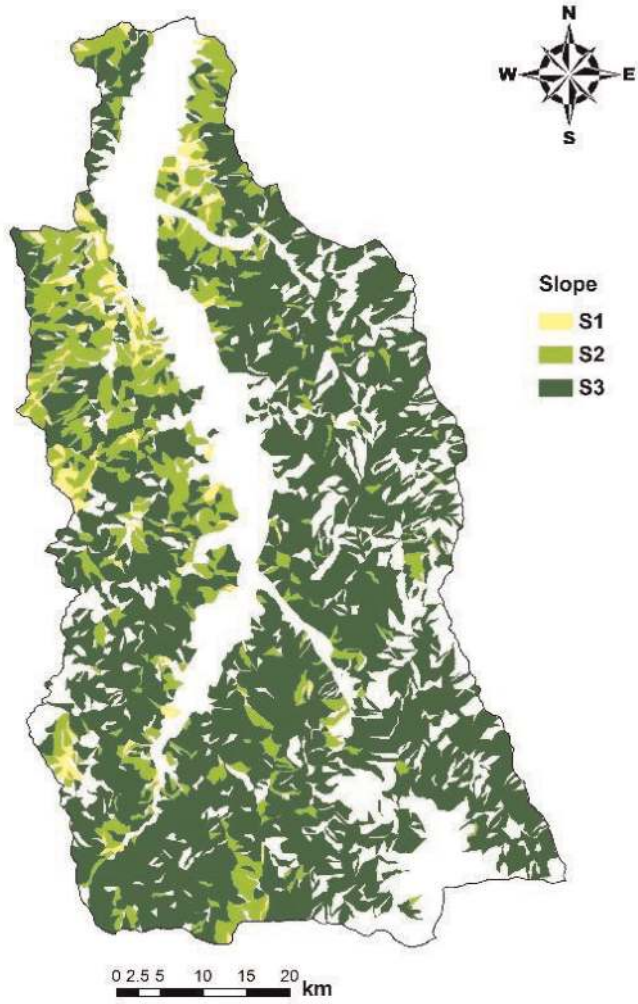

Figure 16.
The slope classification of Chen-Yu-Lan watershed.

association with the slope classification, the determination of landslide of a given slope unit was decided based on the following criteria:

1. Slope S1: the slope unit is counted as a landslide when its landslide area ratio (LAR) is equal to or higher than 5% or the projected landslide area on the slope is greater than 2800 m^2 (0.28 ha). Otherwise, the slope unit is not counted as a landslide area.

2. Slope S2: the slope unit is counted as a landslide when its landslide area ratio is equal to or higher than 5% or the projected landslide area on the slope is greater than 2400 m^2 (0.24 ha). Otherwise, the slope unit is not counted as a landslide area.

3. Slope S3: the slope unit is counted as a landslide when its landslide area ratio is equal to or higher than 5% or the projected landslide area on the slope is greater than 2200 m^2 (0.22 ha). Otherwise, the slope unit is not counted as a landslide area.

The landslide area classification of Chen-Yu-Lan watershed is shown in **Figure 23**. There were 1810 slope units of landslide after Typhon Sinlaku and 1544 ones after Typhoon Morakot, as shown in colored slope units in **Figure 23**.

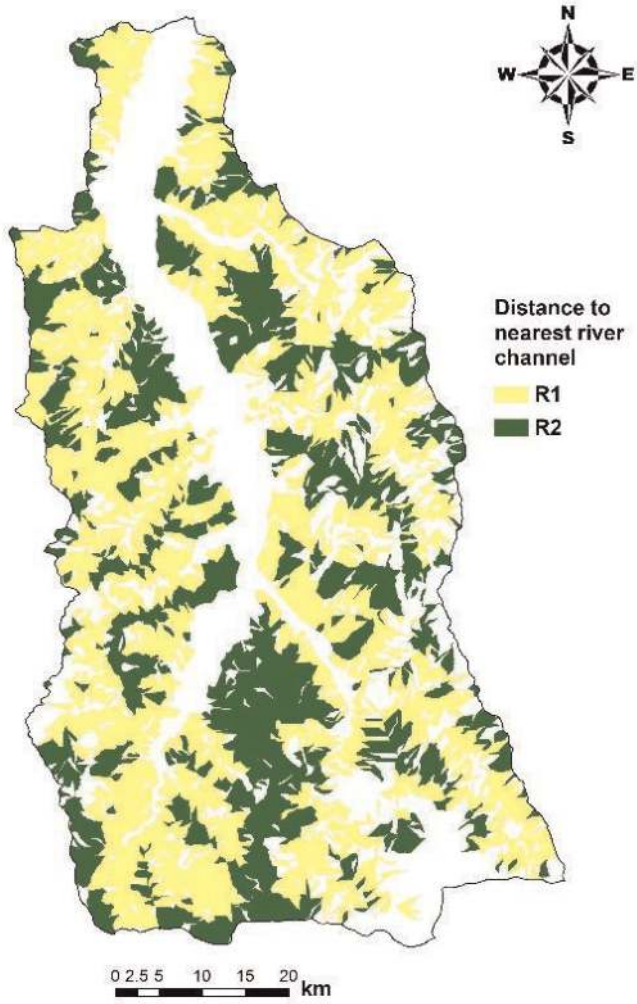

Figure 17.
The classification of distance to the river of Chen-Yu-Lan watershed.

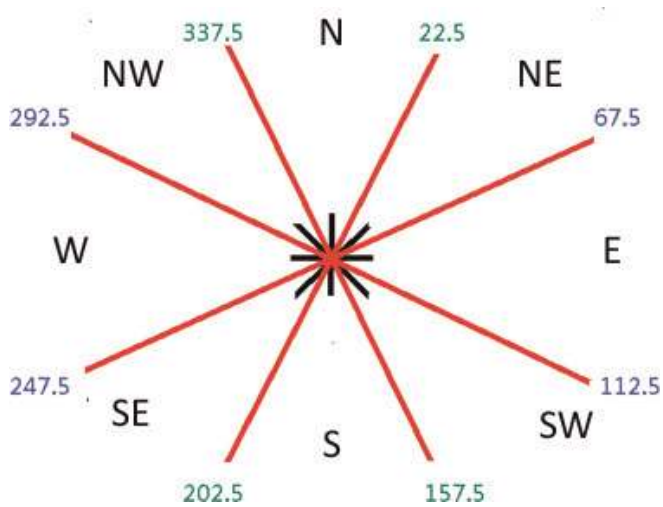

Figure 18.
The slope aspects.

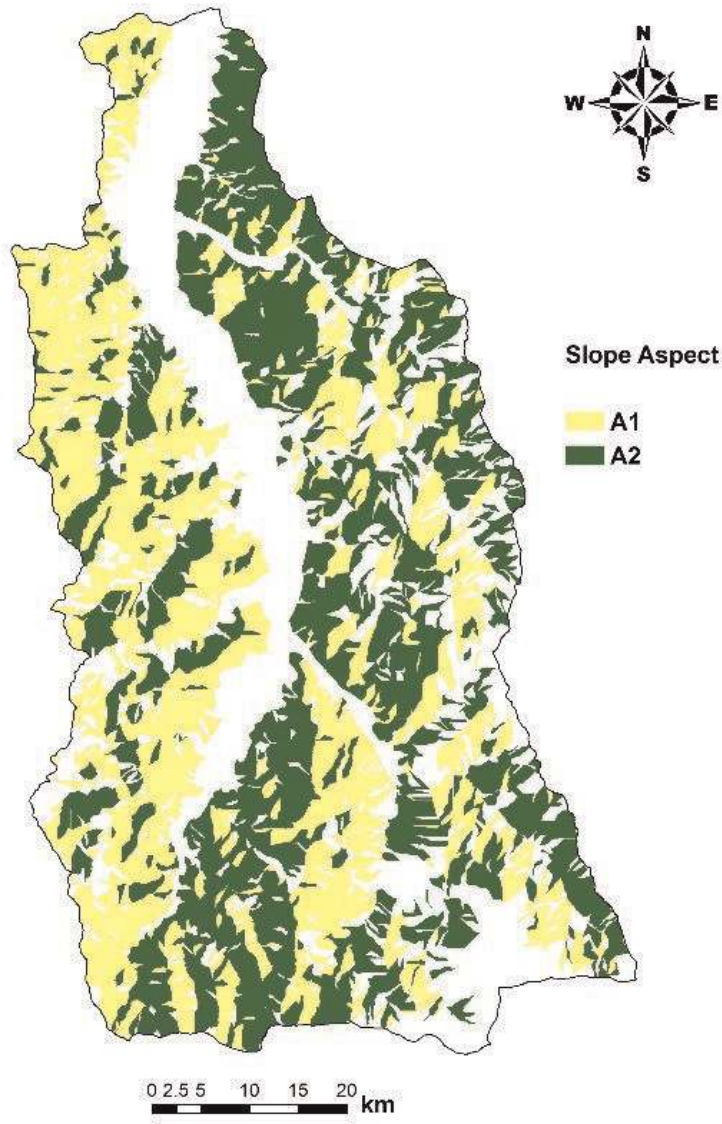

Figure 19.
The slope aspect classification of Chen-Yu-Lan watershed.

4.3 The LFC of Chen-Yu-Lan watershed

The environmental database and rainfall data of typhoon events were applied to classify the slope units and the landslide areas. With the classification described in previous sections, there were a total of 48 classes with combinations of factors G, S, A, R, and N. Each classification was in association with two rainfall indices, the rainfall intensity and effective accumulated rainfall. The fragility of landslide, or the probability of exceeding a level of hazard, was constructed and used for landslide potential assessment. **Tables 9** and **10** summarized the fragility parameters obtained from the two events, and some examples of fragility curves were shown in **Figure 24**. It should be noted that during the classification, insufficient samples of certain classification had led to difficulty of finding parameters needed. Therefore, these samples were combined with other classifications in order to get reasonable probability values of median and standard deviation.

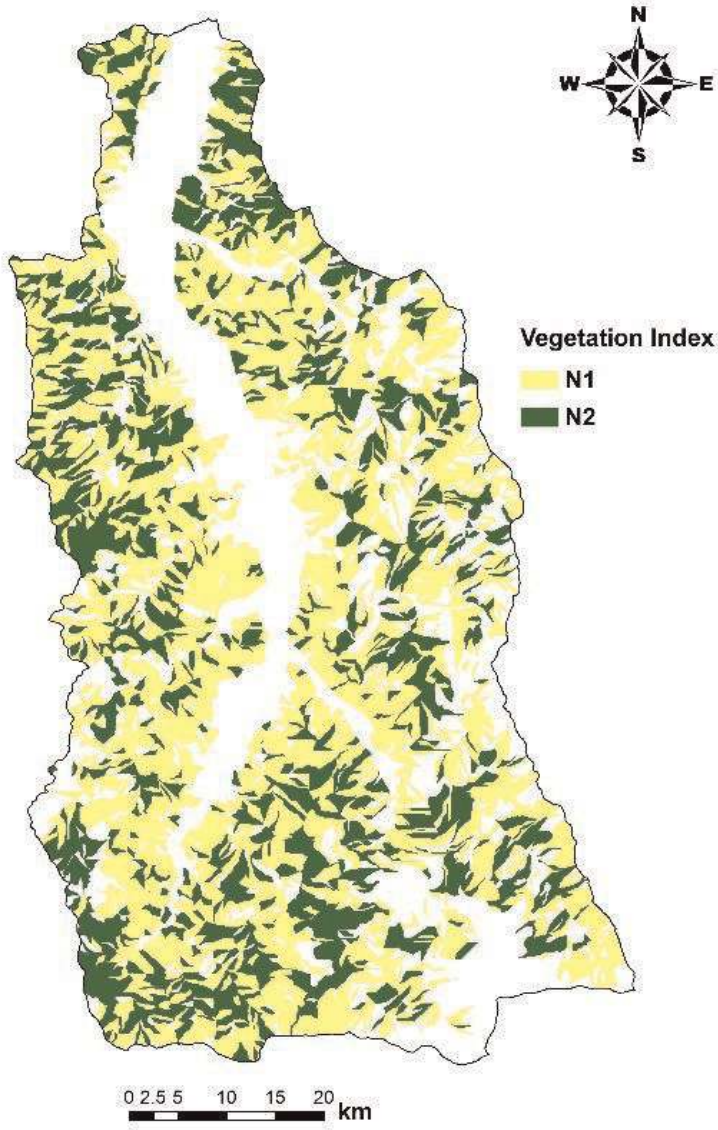

Figure 20.
The vegetation index classification of Chen-Yu-Lan watershed.

4.4 The LFC of Shenmu area

The fragility curves of 48 classification slope units represented the local environmental characteristics of a given area. Instead of directly using 48 set fragility curves, it should be practical to obtain one set of representative fragility curve for a given site or location. To achieve this goal, the weighted fragility curves were introduced and applied to the Shenmu village. The weighted fragility parameters were determined using the following equations:

$$c_{x,m} = \sum_{i=1}^{m} w_i \times c_{xi}, c_{y,m} = \sum_{i=1}^{m} w_i \times c_{yi} \tag{5}$$

$$\zeta_{x,m} = \sqrt{\sum_{i=1}^{m} (w_i \times \zeta_{xi})^2}, \zeta_{y,m} = \sqrt{\sum_{i=1}^{m} \left(w_i \times \zeta_{yi}\right)^2} \tag{6}$$

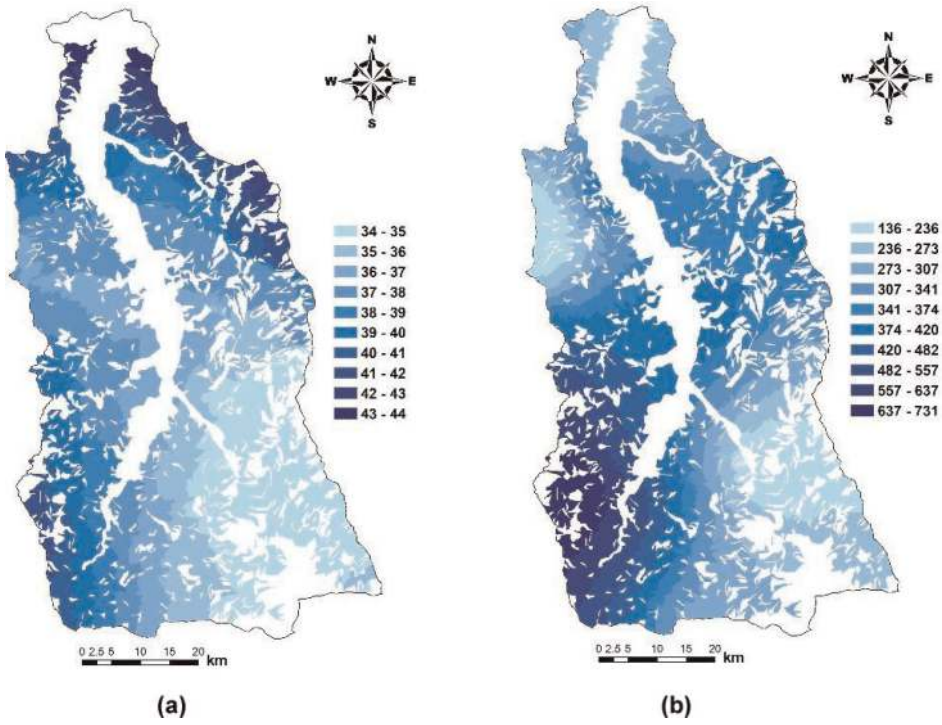

Figure 21.
The rainfall of Chen-Yu-Lan watershed during Typhoon Sinlaku: (a) max. hourly rainfall (I_{max}) and (b) effective accumulated rainfall (R_{te}).

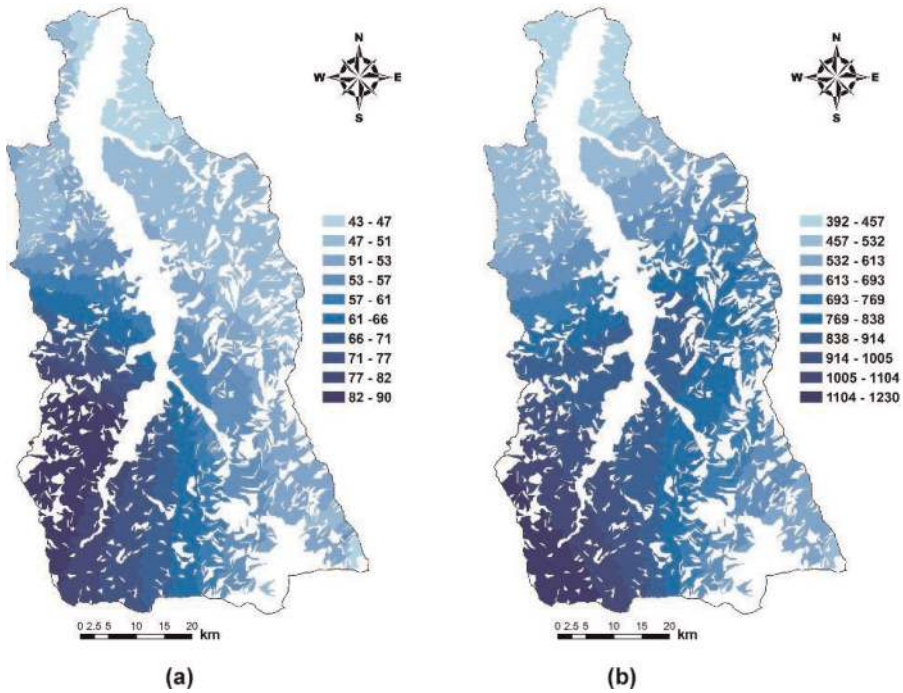

Figure 22.
The rainfall of Chen-Yu-Lan watershed during Typhoon Morakot: (a) max. hourly rainfall (I_{max}) and (b) effective accumulated rainfall (R_{te}).

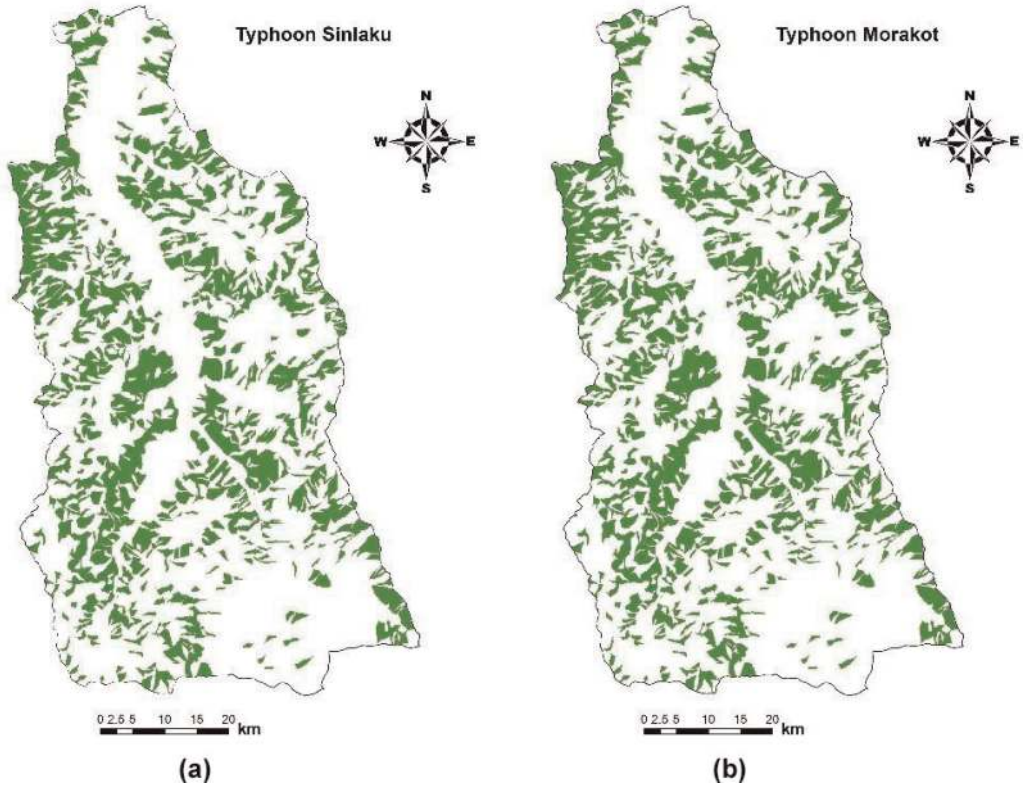

Figure 23.
The landslide area of Chen-Yu-Lan watershed during (a) Typhoon Sinlaku and (b) Typhoon Morakot.

Classification	I_{max} (mm)		R_{te} (mm)		Combined with*
	Median	Std. deviation	Median	Std. deviation	
G1S1A1R1N1	64.40	0.21	485.00	0.28	With 21111
G1S1A1R1N2	27.53	1.24	383.77	0.29	With 21112
G1S1A1R2N1	33.70	0.31	1112.62	0.10	With 21121
G1S1A1R2N2	37.94	0.16	239.39	0.27	With 21122
G1S1A2R1N1	44.40	1.10	290.86	0.24	With 21211
G1S1A2R1N2	43.91	0.16	1007.19	0.71	With 21212
G1S1A2R2N1	32.48	0.77	320.60	0.39	With 21221
G1S1A2R2N2	40.58	0.45	332.07	0.22	With 21222
G1S2A1R1N1	40.44	0.58	235.49	0.79	With 22111
G1S2A1R1N2	72.70	0.32	384.00	0.67	With 22112
G1S2A1R2N1	22.60	0.34	407.35	0.26	With 22121
G1S2A1R2N2	74.16	1.17	527.59	1.20	With 22122
G1S2A2R1N1	22.41	0.70	399.60	1.23	With 22211
G1S2A2R1N2	42.39	0.28	252.25	0.62	With 22212
G1S2A2R2N1	14.08	0.11	706.36	0.80	With 22221
G1S2A2R2N2	115.74	0.61	207.21	0.77	With 22222
G1S3A1R1N1	18.81	0.21	135.69	1.06	

Classification	I_{max} (mm)		R_{te} (mm)		Combined with*
	Median	Std. deviation	Median	Std. deviation	
G1S3A1R1N2	14.51	0.12	295.58	0.29	
G1S3A1R2N1	75.05	0.29	225.74	0.88	
G1S3A1R2N2	28.07	0.38	269.76	0.55	
G1S3A2R1N1	35.79	0.57	967.74	0.35	
G1S3A2R1N2	44.53	1.54	554.12	1.26	
G1S3A2R2N1	29.66	0.72	298.05	0.30	
G1S3A2R2N2	34.00	0.89	269.00	0.69	

Due to the insufficient data, some classifications were combined together in order to obtain reasonable parameters.

Table 9.
Fragility parameters of G1 classification.

Classification	I_{max} (mm)		R_{te} (mm)	
	Median	Std. deviation	Median	Std. deviation
G2S1A1R1N1	64.40	0.21	485.00	0.28
G2S1A1R1N2	27.53	1.24	383.77	0.29
G2S1A1R2N1	33.70	0.31	1112.62	0.10
G2S1A1R2N2	37.94	0.16	239.39	0.27
G2S1A2R1N1	44.40	1.10	290.86	0.24
G2S1A2R1N2	43.91	0.16	1007.19	0.71
G2S1A2R2N1	32.48	0.77	320.60	0.39
G2S1A2R2N2	40.58	0.45	332.07	0.22
G2S2A1R1N1	40.44	0.58	235.49	0.79
G2S2A1R1N2	72.70	0.32	384.00	0.67
G2S2A1R2N1	22.60	0.34	407.35	0.26
G2S2A1R2N2	74.16	1.17	527.59	1.20
G2S2A2R1N1	22.41	0.70	399.60	1.23
G2S2A2R1N2	42.39	0.28	252.25	0.62
G2S2A2R2N1	14.08	0.11	706.36	0.80
G2S2A2R2N2	115.74	0.61	207.21	0.77
G2S3A1R1N1	16.70	0.13	604.42	0.53
G2S3A1R1N2	72.54	0.58	305.93	0.41
G2S3A1R2N1	21.81	1.31	387.14	0.84
G2S3A1R2N2	56.01	1.07	527.88	0.69
G2S3A2R1N1	23.20	0.78	378.00	0.66
G2S3A2R1N2	14.50	0.11	151.30	0.10
G2S3A2R2N1	23.76	0.66	270.92	0.28
G2S3A2R2N2	29.86	1.02	249.28	0.80

Table 10.
Fragility parameters of G2 classification.

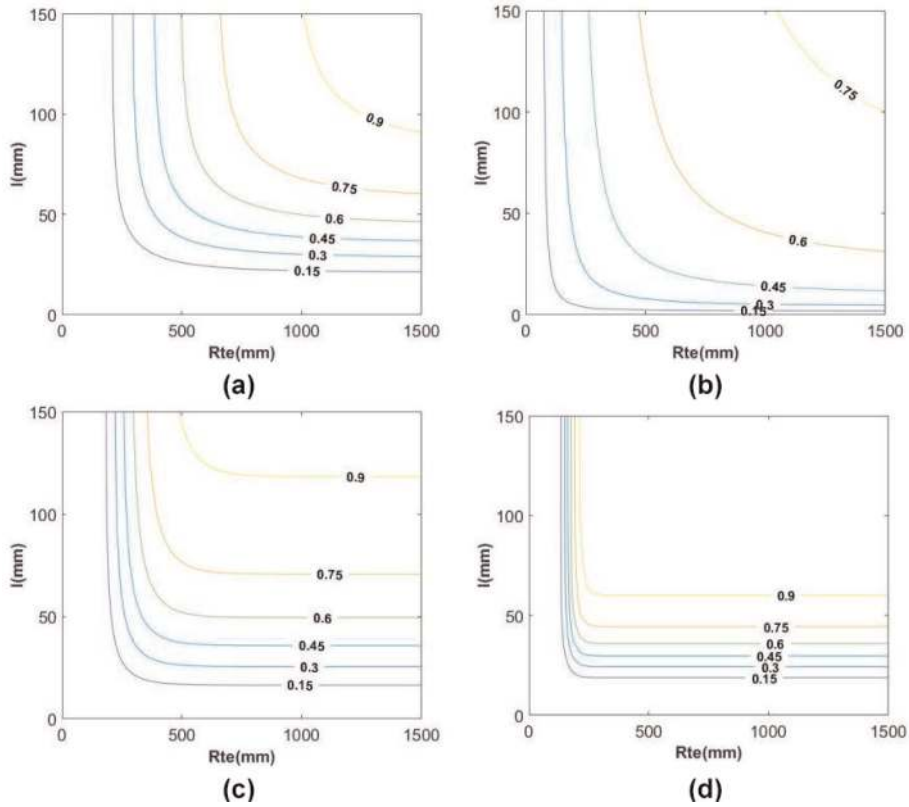

Figure 24.
Examples of fragility curves of Chen-Yu-Lan watershed: (a) G1S3A1R1N1, (b) G2S2A1R1N1, (c) G1S3A1R2N1, and (d) G2S3A1R2N1.

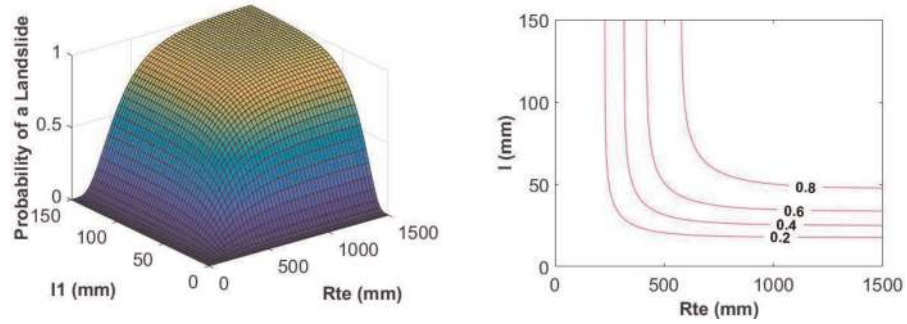

Figure 25.
The fragility surface and fragility curves of Shenmu area.

$$w_i = \frac{n_i}{N_i} \tag{7}$$

where x and y are rainfall indices, $c_{x,\,m}$ and $c_{y,\,m}$ are the weighted median values, $\zeta_{x,\,m}$ and $\zeta_{y,\,m}$ are weighted standard deviation, m is the number of classifications, w_i is the weighting factor of a classification, n_i is the number of slope units of a given classification, and N_i is the total number of slope units.

After the weighted calculation, the fragility parameters of Shenmu area are median $I_{max} = 33$ mm and median $R_{te} = 413$ mm. **Figure 25** shows the weighted fragility curves of Shenmu area.

5. Case studies and results

The risk of landslide was demonstrated by using the critical values of rainfall hazard and landslide fragility. The concept of landslide warning was adopted in this study, and by combining both *Hc* and *Fc*, the warning status includes safe stage and unsafe stages, as illustrated in **Figure 26**. It should be noted that there are two stages of unsafe status, Red I and Red II. Red I stage indicates that the situation has pass *Hc* and a rainfall hazard could occur. Red II stage implies the most serious condition that in addition to the rainfall hazard, a landslide could occur as well. Both stages are determined with a probability when given a rainfall condition. The procedure of determining safe stage was designed to match the needs of disaster preparation and prediction of government.

Cases of landslides and debris flows in Shenmu were collected from the disaster notices issued by Soil and Water Conservation Bureau of Taiwan. As shown in **Table 11** and **Figure 27**, a total of seven cases were used to determine the critical values of *Hc* (=0.91) and *Fc* (=0.23) of Shenmu. These cases were used in the assumption that whenever there was a debris flow, there should be landslides at the upper stream areas before or during the debris flow.

The rainfall history of Typhoon Morakot in 2009 and 0601 Heavy Rainfall in 2016 were used to evaluate the landslide risk assessment in Shenmu. **Figure 28**

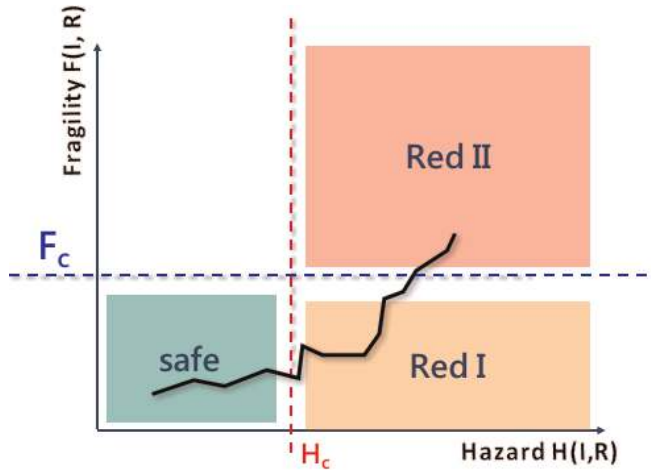

Figure 26.
The warning conditions based on landslide fragility (Fc) and rainfall hazard (Hc).

Year	Event	Disaster	Village	I_{max} (mm)	R_{te} (mm)
2009	Typhoon Morakot	Debris flow, flood	Tongfu	85.5	1130
2009	Typhoon Morakot	Debris flow	Wangmei	85.5	1130
2009	Typhoon Morakot	Landslide	Shenmu	47.5	829.5
2009	Typhoon Morakot	Debris flow	Shenmu	42.5	750
2009	Typhoon Morakot	Debris flow	Shenmu	33.5	641
2009	Typhoon Morakot	Landslide	Shenmu	20	476.5
2009	Typhoon Morakot	Debris flow	Shenmu	38.5	877
2012	0610 Heavy rainfall	Debris flow, flood	Shenmu	18.5	450.6

Table 11.
The disaster notices around Shenmu area.

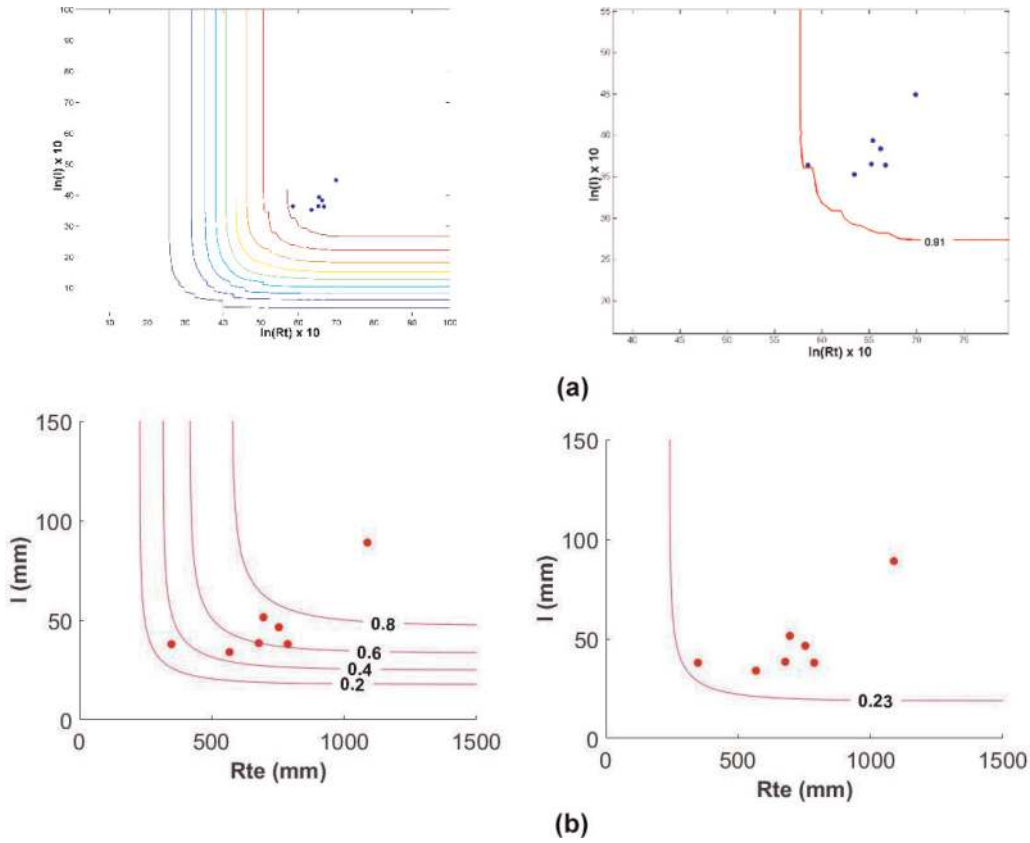

Figure 27.
The probability thresholds of rainfall hazard and landslide fragility in Shenmu area: (a) rainfall warning threshold and (b) landslide warning threshold.

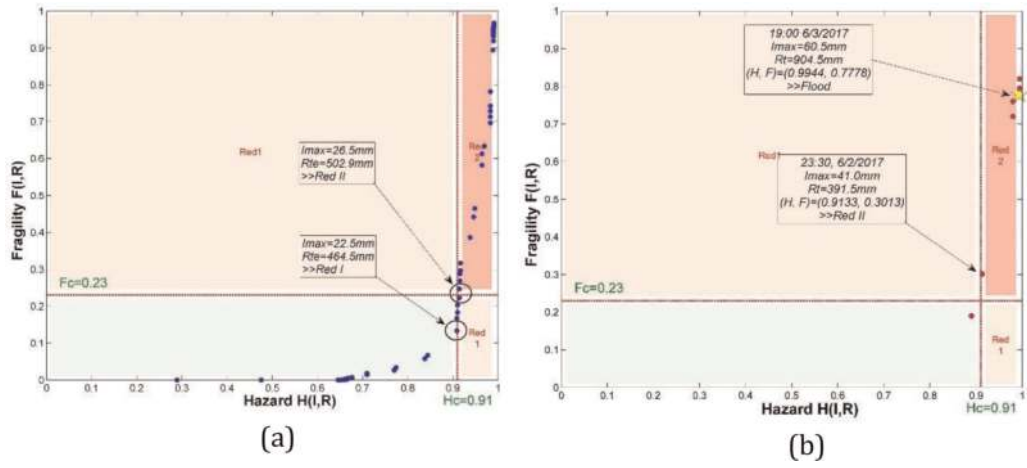

Figure 28.
The change of probability in Shenmu area during (a) Typhoon Morakot (2009) event and (b) 0601 heavy rainfall in 2016 (after [4, 5]).

shows the results of event, and the dots in the figure represent the rainfall condition (hourly rainfall and cumulative rainfall) and the probability of hazard. It was noted that the dots behaved like a "snake" line going from Safe stage to Red I and Red II stages. Also, the snake line stayed shortly at Red I stage for both events and passed to Red II in a jump. This condition implied that when the situation was beyond the *Hc* line, the landslide hazard was very likely to occur. The results conformed to the

records of Typhoon Morakot. Severe landslides occurred at the upper stream areas in Shenmu during the typhoon. Therefore, the proposed risk assessment and warning stages of landslide were reasonably useful in this case.

6. Summary and conclusions

This study had developed the landslide fragility curve model by using the spatial data and statistical methods. The fragility curves of the study area were derived for all combinations of environmental and triggering factors. The data sets included the geomorphological and vegetation condition factors, based on the landslides at the Chen-Yu-Lan watershed in Taiwan, during Typhoon Sinlaku (September 2008) and Typhoon Morakot (August 2009). This study also proposed landslide risk assessment using rainfall hazard potential and landslide fragility curves and concluded findings as follows:

1. Overall, the proposed model provides considerably accurate and reliable results on landslide estimations in terms of spatial distribution.

2. Adoption of slope unit was physically proper in modeling landslide locations.

3. The classifications of slope unit can be applied to different areas, and the fragility curve of each classification can be used directly.

4. The procedure of risk assessment was useful for practical landslide disaster preparation and prediction.

5. The LFC model was developed using two typhoon events. More events and landslide cases are needed to improve the LFC model in the future. Furthermore, the classification of upstream areas based on their environment is suggested for better possible estimation.

6. The applicability of factors should be considered before developing the model. The concerns about the model factors and the limits of satellite images can be resolved by using different methods to obtain necessary data. For example, the information of LIDAR may be used with the satellite images to provide better description on landslide identification. Therefore, the LFC model could be improved when more factors are available and applicable.

Acknowledgements

The authors would like to express their gratitude to research assistant Xingping Wang, for helping in collecting all the data relevant to the landslides in the Chen-Yu-Lan watershed. The authors also would like to thank the Soil and Water Conservation Bureau in Taiwan for supporting this research.

DOI: http://dx.doi.org/10.5772/intechopen.89183

Author details

Yi-Min Huang[1*], Tsu-Chiang Lei[2], Bing-Jean Lee[1] and Meng-Hsun Hsieh[1]

1 Department of Civil Engineering, Feng Chia University, Taichung, Taiwan

2 Department of Urban Planning and Spatial Information, Feng Chia University, Taichung, Taiwan

*Address all correspondence to: ninerh@mail.fcu.edu.tw

References

[1] Dilley M, Chen RS, Deichmann U, Lerner-Lam AL, Arnold M, Agwe J, et al. Natural Disaster Hotspots: A Global Risk Analysis (English). Washington, DC: World Bank. Available from: http://documents.worldbank.org/curated/en/621711468175150317/Natural-disaster-hotspots-A-global-risk-analysis; 2005

[2] Lei TC, Huang YM, Lee BJ, Hsieh MH, Lin KT. Development of an empirical model for rainfall-induced hillside vulnerability assessment: A case study on Chen-Yu-Lan Watershed, Nantou, Taiwan. Natural Hazards. 2014; **74**:341-373

[3] Lee BJ, Lei TC, Huang YM, Hsieh MH. 2015 Application of Landslide Fragility Curves in Landslide Risk and Warning Criteria, Project Report. Soil and Water Conservation Bureau, Taiwan (in Chinese). 2016. p. 341

[4] Lee BJ, Lei TC, Huang YM, Hsieh MH. 2016 Application of Landslide Fragility Curves in Landslide Risk and Warning Criteria, Project Report. Soil and Water Conservation Bureau, Taiwan (in Chinese). 2017. p. 224

[5] Lee CY et al. Risk assessment of landslide by using fragility curves: A case study in Shenmu, Taiwan. In: Proceedings of the 5th International Conference on Geotechnical Engineering for Disaster Mitigation and Rehabilitation (5th GEDMAR); 14–17 December 2005; Taipei, Taiwan: Airiti Press Inc. 2017. pp. 137-148

[6] Pradhan B, Lee S. Delineation of landslide hazard areas on Penang Island, Malaysia, by using frequency ratio, logistic regression, and artificial neural network models. Environmental Erath Science. 2009;**60**(5):1037-1054

[7] Lei TC, Wan S, Chou TY, Pai HC. The knowledge expression on debris flow potential analysis through PCA +LDA and rough sets theory: A case study of Chen-Yu-Lan Watershed, Nantou, Taiwan. Environmental Earth Sciences. 2011;**63**(5):981-997

[8] Wan S, Lei TC, Chou TY. A landslide expert system: Image classification through integration of data mining approaches for multi-category analysis. International Journal of Geographical Information Science. 2012;**26**:747-770

[9] Soil and Water Conservation Bureau. Soil and Water Conservation Handbook. Taiwan: Soil and Water Conservation Bureau; 2016. Available from: https://drive.google.com/file/d/1FzwMzkd_12qzGhOGjcQX7F-x2ihHvr6e/view

[10] Lillesand TM, Kiefer RW. Remote Sensing and Image Interpretation. New York: John Wiley and Sons; 1999. 736 p

[11] Bannari A, Morin D, Bonn F, Huete AR. A review of vegetation indices. Remote Sensing Reviews. 1995; **13**:95-120

[12] Xie M, Esaki T, Zhou G. GIS-based probabilistic mapping of landslide hazard using a three-dimensional deterministic model. Natural Hazards. 2004;**33**:265-282. DOI: 10.1023/B:NHAZ.0000037036.01850.0d

[13] Shinozuka M, Feng MQ, Lee J, Naganuma T. Statistical analysis of fragility curves. ASCE Journal of Engineering Mechanics. 2000;**126**(12): 1224-1231

[14] Hsieh MH, Lee BJ, Lei TC, Lin JY. Development of medium- and low-rise reinforced concrete building fragility curves based on Chi-Chi Earthquake data. Natural Hazards.2013;**69**(1):695-728. DOI: 10.1007/s11069-013-0733-8

[15] AECOM. A study of sediment management policies on climate change for river basins in southern

Taiwan- Gaoping river case study. Project Report. Water Resources Planning Institute, Water Resources Agency, Ministry of Economic Affairs, Taiwan. 2011. 342 p. Available from: https://www.wrap.gov.tw/library_1.aspx?id=22547 Accessed: 19 July 2019]